

Geological implications of a physical libration on Enceladus

T.A. Hurford^{a,*}, B.G. Bills^{b,c}, P. Helfenstein^d, R. Greenberg^e, G.V. Hoppa^f, D.P. Hamilton^g

^a Planetary Systems Laboratory, NASA Goddard Spaceflight Center, Greenbelt, MD 20771, USA

^b Jet Propulsion Laboratory, Pasadena, CA 90119, USA

^c Institute for Geophysics and Planetary Physics, Scripps Institution of Oceanography, La Jolla, CA 92093, USA

^d CRSR, Cornell University, Ithaca, NY 14853, USA

^e Lunar and Planetary Laboratory, University of Arizona, Tucson, AZ 85721, USA

^f Raytheon, Woburn, MA 01801, USA

^g Department of Astronomy, University of Maryland, College Park, MD 20742, USA

ARTICLE INFO

Article history:

Received 20 October 2008

Revised 16 March 2009

Accepted 17 April 2009

Available online 21 May 2009

Keywords:

Tectonics

Enceladus

ABSTRACT

Given the non-spherical shape of Enceladus [Thomas et al., 2007], the satellite will experience gravitational torques that will cause it to physically librate as it orbits Saturn. Physical libration would produce a diurnal oscillation in the longitude of Enceladus' tidal bulge, which could have a profound effect on the diurnal tidal stresses experienced by the surface of the satellite. Although Cassini ISS has placed an observational upper limit on the amplitude of Enceladus' libration, smaller amplitudes can still have geologically significant consequences. Here we present the first detailed description of how physical libration affects tidal stresses and how those stresses might then affect geological processes including crack formation and propagation, south polar eruption activity, and tidal heating. Our goal is to provide a framework for testing the hypothesis that geologic features on Enceladus are produced by tidal stresses from diurnal librations of the satellite.

Published by Elsevier Inc.

1. Introduction

The Cassini spacecraft observed plumes actively erupting from the south polar region of Enceladus (Porco et al., 2006), and the heat emanating from the south polar region has been estimated to be ~ 6 GW (Spencer et al., 2006). This came as quite a surprise since this small moon of Saturn (Radius = 252 km) was expected to have cooled long ago, based on estimates of heating within the satellite. These estimates place current radiogenic heating at 0.32 GW (Schubert et al., 1986; Porco et al., 2006) and tidal heating from its small orbital eccentricity ($e = 0.0047$) at just 0.12 GW if the Love number describing Enceladus' gravitational response to the tide-raising potential, k_2 , is 0.0018 and the tidal dissipation factor, Q , is 20 (Yoder, 1979; Porco et al., 2006). Together these two sources of heating provide only about 0.4 GW, less than a tenth of the observed heat emanating from the south pole.

However, the estimates of tidal heating rely on the assumed tidal response of Enceladus that may be too conservative, so tidal heating may be greater than expected. In fact, recent work by Hurford et al. (2007) and Nimmo et al. (2007) require a larger tidal deformation of Enceladus in order to produce sufficient tidal stress

to open cracks on the surface and generate heat through tidal shearing. This larger tidal response implies k_2 must be at least 0.12, implying at least 8 GW of tidal heating (for $Q = 20$). Even though this amount of heating might be sufficient to explain the ~ 6 GW observed at the south pole, it is a global budget and therefore it is unlikely that most of this tidal heating would be focused in a region near the south pole.

Thus, the predicted amount of tidal heating seems to be insufficient to drive the plume activity we observe from Enceladus' south pole. However, there may be mechanisms that can enhance tidal heating still further. Even more heat could be tidally dissipated by a physical libration of Enceladus as it orbits Saturn (Wisdom, 2004). Cassini scientists sought evidence of a physical libration and placed an upper limit on its amplitude. Librations smaller than the Cassini limit remain possible, however, and even small librations can dramatically increase tidal heating as we show below and may be the key to reconciling Enceladus heat budget deficit. Accordingly, we proceed with an investigation of the many ramifications of physical librations.

2. Tidal stress on a librating body

Enceladus' finite orbital eccentricity causes small daily changes in the distance between Enceladus and Saturn, affecting the height

* Corresponding author.

E-mail address: terry.a.hurford@nasa.gov (T.A. Hurford).

of the tide raised on the satellite by the planet. During an orbit, the height of the main tide oscillates with an amplitude $(9eh_2MR)/(4\pi\rho_{av}a^3)$ where e is the orbital eccentricity h_2 is the Love number describing the radial response of the body to the tide raising potential, M is the mass of the tide-raiser in this case Saturn, R is Enceladus' radius, ρ_{av} is the average density of Enceladus and a is the semi-major axis of its orbit, which describes the average distance to Saturn.

Besides affecting the height of the tide on Enceladus, the orbital eccentricity also causes the longitude of the tidal bulge to oscillate as it tracks the position of Saturn throughout an orbit. This oscillation is called the “optical libration” in longitude. The term was coined by Isaac Newton to describe the apparent change in longitude of features on the Moon as described by Galileo in 1637 (Newton, 1686).

Even if the eccentricity were zero, a moon could experience a “physical libration” or an actual wobble of the moon about its own center of gravity. This physical libration would also result in the oscillation of the tidal bulge in longitude with respect to a fixed location. The physical libration is composed of both a free and forced component.

The free libration period of Enceladus depends on the shape of the satellite and the distribution of mass within its interior. Tidal dissipation should have damped this libration to zero amplitude. However if the free libration period is commensurate with the orbital period, a spin-orbit resonance occurs which may increase the amplitude of this libration (Wisdom, 2004). Based on Cassini ISS data of Enceladus' shape, the free libration period is estimated to be about 4 times the orbital period (Porco et al., 2006), implying Enceladus might be in such a spin-orbit resonance. However, for

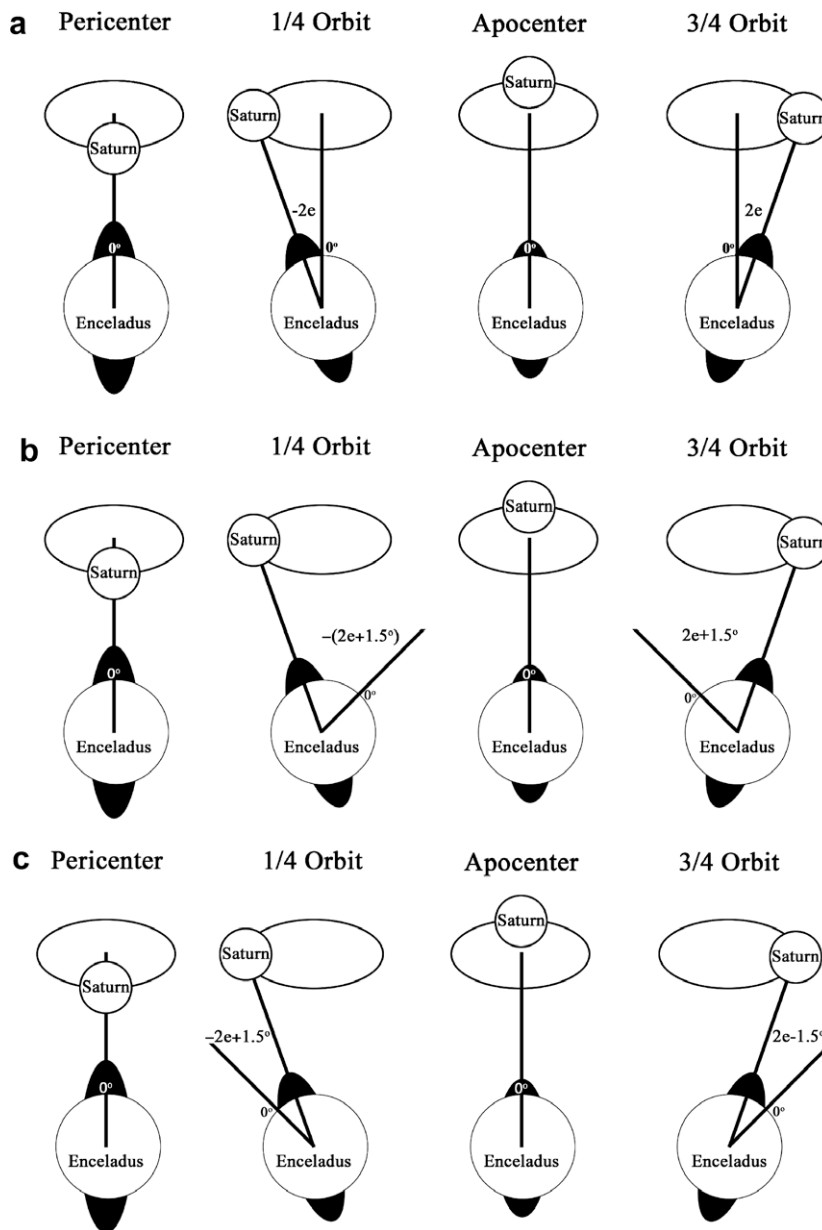


Fig. 1. Sources of stress on Enceladus. The tidal bulge raised on Enceladus by Saturn (in black) changes both its position and its magnitude as the satellite orbits the planet. These effects are shown in a reference frame centered on Enceladus that rotates at the satellite's mean orbital rate n . The variations in the tidal bulge in (a) are due to optical libration. Panel (b) adds to optical libration a hypothetical out-of-phase (phase 180°) physical libration of 1.5° while panel (c) adds an in-phase (phase 0°) physical libration of the same magnitude. Straight lines from Enceladus indicate how the direction to Saturn and the zero point of a longitude grid fixed to Enceladus change with time. While the position of the tidal bulge relative to landmarks on Enceladus depends on both eccentricity and physical libration, the magnitude of the tidal bulge is affected only by the first process. In the special case that Enceladus exhibits an in-phase physical libration with an amplitude of $2e$, the longitude of the tidal bulge is fixed to 0° similar to panel (c).

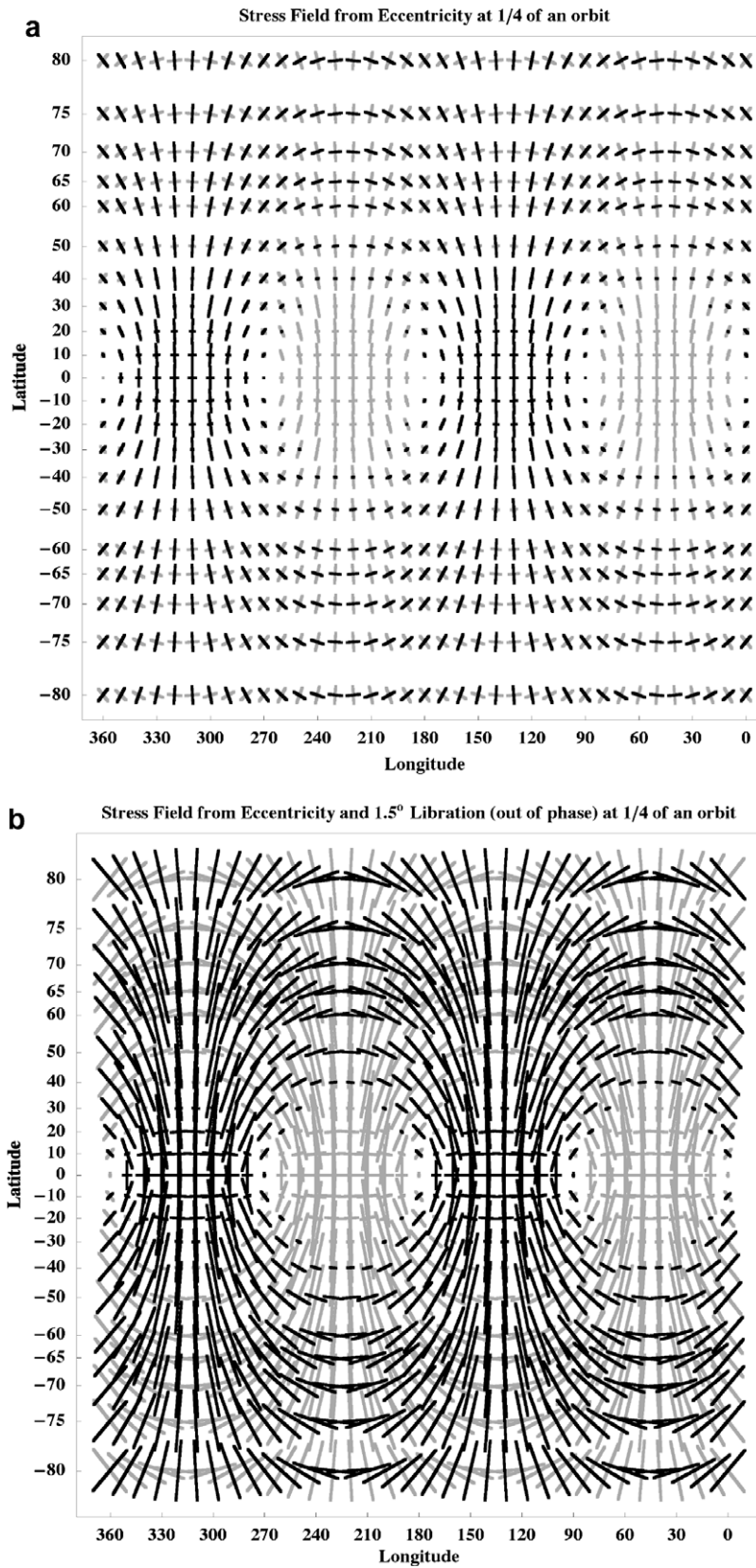


Fig. 2. Here we illustrate the tidal stress on Enceladus 1/4 of an orbit past pericenter ($nt = \pi/2$) for the three cases of Fig. 1. Dark lines represent tension, while lighter lines show compression. As in Fig. 1, (a) corresponds to the optical libration of the tide due solely to Enceladus' orbital eccentricity. To this, we add in (b) an out-of-phase physical libration with amplitude of 1.5° and in (c) an in-phase 1.5° physical libration. With an in-phase physical libration of amplitude $2e$, the positions of the tidal bulges are fixed on Enceladus and stresses arise only from their amplitude variations. The stress fields at ($nt = 3\pi/2$) can be obtained from the ones shown here by interchanging the meaning of the dark and light lines, so that the former represents compression while the latter shows tension.

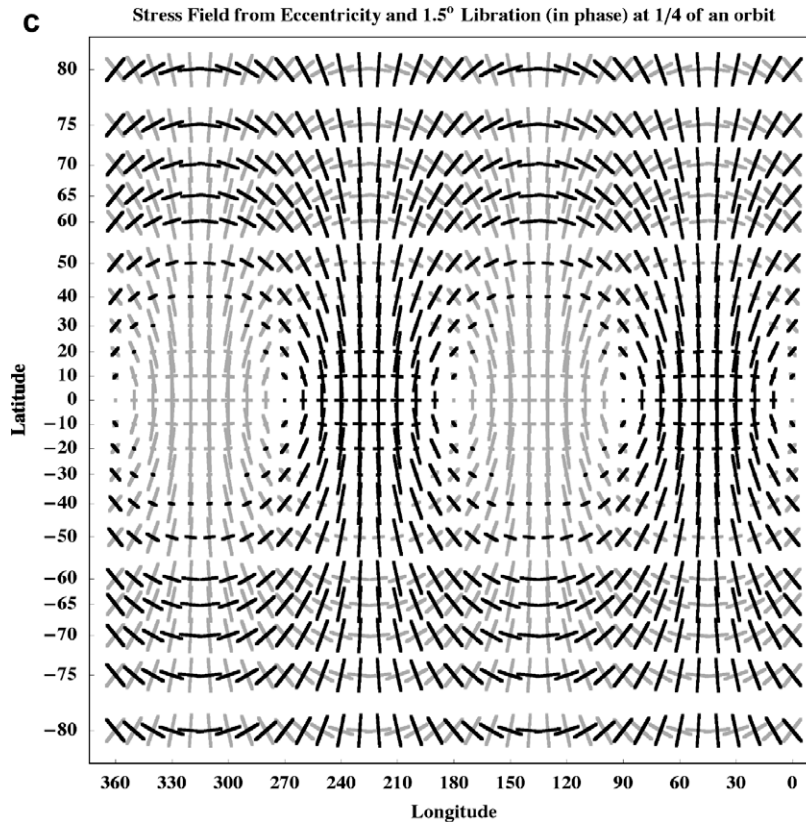


Fig. 2 (continued)

this paper we assume that the free libration has been damped to zero amplitude.

The other component of the physical libration, the forced libration, is driven by torques from Saturn on the surface of the satellite. Enceladus' forced libration responds at the frequency of the forcing, which would likely be the satellite's orbital mean motion n . The amplitude of the forced libration depends on the interior properties of the satellite. Moreover, if the icy crust of Enceladus is decoupled from the deeper interior by a liquid layer, a larger forced libration amplitude may be possible. To the extent that tidal heating influences the mean thickness and lateral variation in local thickness of the ice shell, the amplitude and phase of the forced libration may likely change over time.

To simplify calculations and to approximate the surface stresses from the tidal deformation of an elastic outer layer, we assume that the icy shell is thin and that it is decoupled from the deeper interior of Enceladus. In our model there is negligible shear between the thin elastic shell and the interior, which can be caused by the presence of a global ocean (Sohl et al., 2006; Zhang and Nimmo, 2009). The elastic outer layer cannot affect the tidal distortion of Enceladus and thus it deforms to fit the tidal figure taken by Enceladus, stretching and producing stress on its surface. These stresses are given by the Vening–Meinesz equations:

$$\sigma_{\theta\theta} = -\frac{3Mh_2\mu}{8\pi\rho_{av}a^3} \left(\frac{1+\nu}{5+\nu}\right) (5 + 3\cos 2\theta) \quad (1)$$

and

$$\sigma_{\phi\phi} = \frac{3Mh_2\mu}{8\pi\rho_{av}a^3} \left(\frac{1+\nu}{5+\nu}\right) (1 - 9\cos 2\theta), \quad (2)$$

where θ is a surface point's angular distance from the axis of symmetry with respect to the tidal deformation (Melosh, 1977; Leith

and McKinnon, 1996; Greenberg et al., 1998). In these expressions μ is the rigidity of the thin elastic shell while ν is its Poisson's ratio. The stress along the surface in the direction radial to the axis of symmetry is given by $\sigma_{\theta\theta}$, while $\sigma_{\phi\phi}$ is the stress along the surface in a direction orthogonal to the $\sigma_{\theta\theta}$ stress. In the convention used here positive stresses are compressional and negative stresses tensile.

Note that $\sigma_{\theta\theta}$ is always tensile, while $\sigma_{\phi\phi}$ is tensile for $\theta < 42^\circ$ (near the tidal symmetry axis) and compressional for larger θ . Furthermore note that $\sigma_{\theta\theta} = \sigma_{\phi\phi}$ at $\theta = 0^\circ$ as required by symmetry. The direction of these stresses can be understood from considering tidal deformation which elongates a spherical body to form two bulges at $\theta = 0^\circ$ and $\theta = 180^\circ$ while shrinking the circumference of the great circle at $\theta = 90^\circ$.

The orbital eccentricity (optical libration) and rotational (physical libration) effects combine, yielding the diurnal, or daily, oscillation of the tide, as illustrated schematically in Fig. 1. The longitude of the tidal bulge λ_B , relative to a fixed point on the surface, at any point throughout the orbit is the difference between the optical and physical libration or

$$\lambda_B = -2e \sin(nt) + F \sin(nt + \psi), \quad (3)$$

where $2e$ is the amplitude of the optical libration, n is the mean motion, t the time since pericenter passage, and F is the amplitude of the physical libration, which has a phase ψ relative to the optical libration. The amplitude of the oscillation in the longitude of the tidal bulge is described by $L = \sqrt{4e^2 + F^2 - 4eF \cos(\psi)}$. $\psi = 0^\circ$ would minimize L and corresponds to a physical libration that is "in-phase" with the optical libration, while $\psi = 180^\circ$ maximizes L and would be "out-of-phase". The oscillatory motion of the tidal bulge produces daily changes in θ in Eqs. (1) and (2). The changes in θ plus daily changes in the height of the tide combine, yielding the diurnal

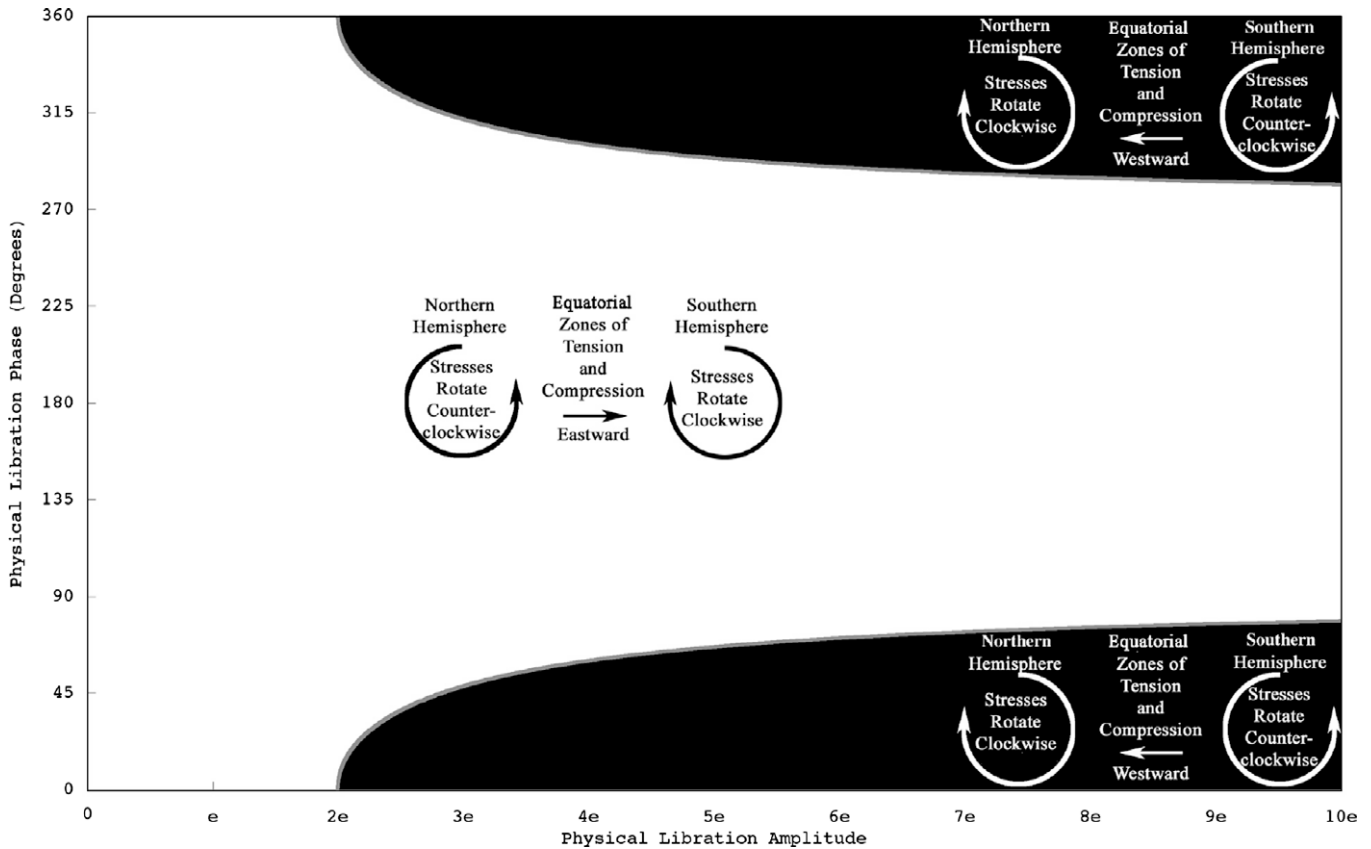


Fig. 3. Here we plot the phase of the physical libration against its amplitude. In the white region, the orientation of the principal tidal stresses rotate in a counterclockwise fashion in the northern hemisphere and clockwise in the southern hemisphere while zones of compression and tension move towards the east along the equator. In the black region that pattern is reversed. Finally, along the gray border between the white and black region, the tidal stress field changes its sense of rotation at pericenter and apocenter and the zones of tension and compression oscillate about a fixed longitude. This figure is general and therefore applicable to any librating satellite.

nally varying part of the tide, producing elastic stress on the surface (see Appendix A).

The three cases illustrated in Fig. 1, have identical tidal stress fields at pericenter and also at apocenter. (c.f. Greenberg et al. (1998), Greenberg (2005)). However, the three stress fields differ when the satellite is at $nt = \pi/2$ as can be seen in Fig. 2. The stresses associated with 1.5° out-of-phase physical librations (Fig. 2b) are enhanced in magnitude relative to case (a) with no physical libration. Although the magnitude of the tidal bulge is the same in both cases, the longitude of the tidal bulge moves further from zero, producing more stress in case (b). For in-phase physical librations (case c), the stresses (Fig. 2c) are enhanced in magnitude and the principle stresses are rotated by 90° . Here the longitude of the tidal bulge is on the opposite side of the 0° meridian, reversing the directions of tension and compression.

For a water–ice crust, we used the plausible values for the elastic parameters of $\mu = 3.52 \times 10^9$ Pa and $\nu = 0.33$ and assumed a conservative value for the tidal response given by h_2 is 0.32, which corresponds to a diurnal tidal amplitude of ~ 5 m when $e = 0.0047$ and $\rho_{av} = 1608$ kg/m³. We assumed this specific value of h_2 because this value yields maximum stresses on the order of 1 bar or 10^5 Pa. On Europa, stresses of this order are thought to control tensile failures in its icy crust (Hoppa et al., 2001; Hurford et al., 2007), and we assume that stresses of this magnitude would also allow for tensile failure on Enceladus.

Fig. 2 shows the tidal stress field at one time during the orbit, but the tidal stress field is constantly changing. In the case in which the satellite exhibits no physical libration, zones of tension and compression at the equator move eastward throughout the orbit. Moreover, the orientation of the principle stresses rotate in a counterclockwise fashion in the northern hemisphere and clockwise in

the southern hemisphere. When the amplitude of the physical libration is small compared to the optical libration ($F < 2e$) or the physical libration is out of phase with the optical libration, this pattern of stress change throughout the orbit remains the same as for the optical libration alone, even though the magnitude of the stresses are affected (the white region in Fig. 3). However, when the amplitude of the physical libration is equal to or greater than the amplitude of the optical libration and relatively in phase with the optical libration (the black region in Fig. 3), the zones of tension and compression at the equator move westward throughout the orbit and the orientation of the principle stresses rotate in a clockwise fashion in the northern hemisphere, counterclockwise in the southern hemisphere. In a special case, where the amplitude of the physical libration is exactly equal to the amplitude of the optical libration ($F = 2e$) and in phase with it ($\psi = 0$), the orientation of the principle stresses do not rotate throughout the orbit and the zones of tension and compression remain stationary while oscillating between compression and tension. Along the gray lines in Fig. 3, defined by $\cos \psi = 2e/F$, the tidal stress field changes its sense of rotation at pericenter and apocenter and the zones of tension and compression oscillate about a fixed longitude. It follows from Eq. (3) that the oscillation of the tidal bulge would be at its maximum eastward or westward position at pericenter and apocenter if $\cos \psi = 2e/F$.

3. Effects on tidal processes

Cassini's observational limit on the Enceladus' total libration (i.e. the combined optical and physical libration) is $L \leq 1.5^\circ$ (Porco et al., 2006). Although the upper limit on the libration amplitude

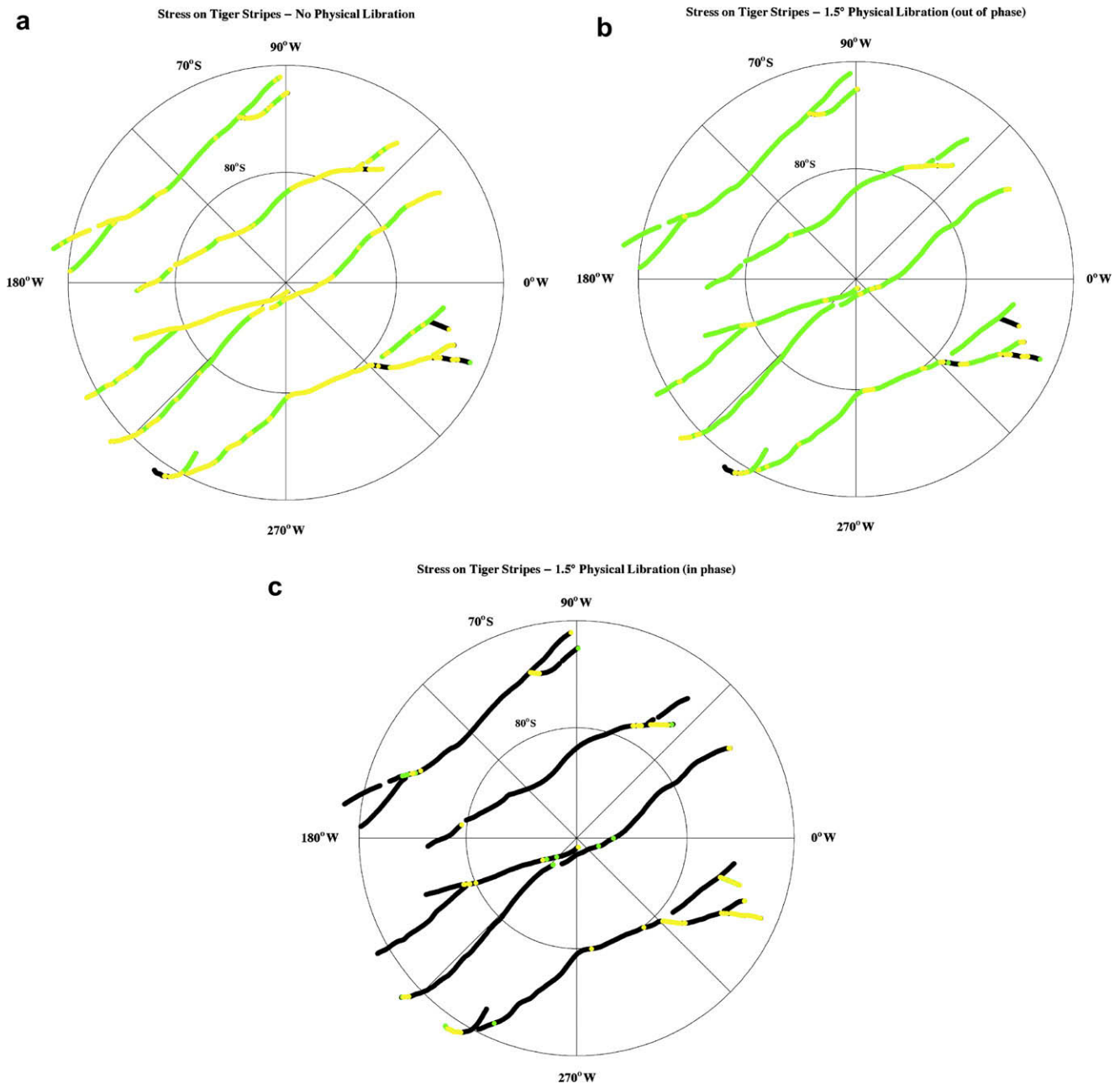


Fig. 4. The stress state across the tiger stripe rifts is shown during the period $\pi/4 < nt < \pi/2$ (second eighth of the orbit) for the cases in Fig. 1a–c. The color indicates the stress state. Black means that portion of the feature was in compression during the entire portion of the orbit while green means that it was in tension. Yellow indicates that the stress switched from compression to tension, opening the rift during this period.

for Enceladus seems small, this libration is comparable to the optical libration and has significant ramifications for the satellite. The physical libration affects the tidal stress and thus will influence all processes in which stress plays a dominant role. Although Enceladus' physical libration may not be directly detectable by Cassini, the effect of the physical libration may be observable, providing indirect evidence of Enceladus' libration state.

3.1. Tidal control of eruptions

In addition to the plumes that were detected near the south polar region of Enceladus, large rifts in the crust were discovered near the south pole, which are evidently the source of the plumes (Porco et al., 2006; Spencer et al., 2006; Spitale and Porco, 2007).

These features informally called “tiger stripes”, exhibit higher temperatures than the surrounding terrain and are likely sources of the observed eruptions (Spencer et al., 2006). By a method developed to consider stress along cracks on Europa (Greenberg et al., 1998; Hoppa et al., 1999a), diurnal variation in the surface stress normal to a fault can be calculated. Over Enceladus' orbital period, stresses across the tiger stripes alternate from compressive to tensile, allowing the faults to open, which could expose a sub-surface volatile reservoir, creating an eruption (Hurford et al., 2007). The state of the stress across the fault depends on the azimuthal orientation (the “strike”) of the fault as well as on its location.

A physical libration changes the stresses on the tiger stripes, especially the timing of the transition between tension and

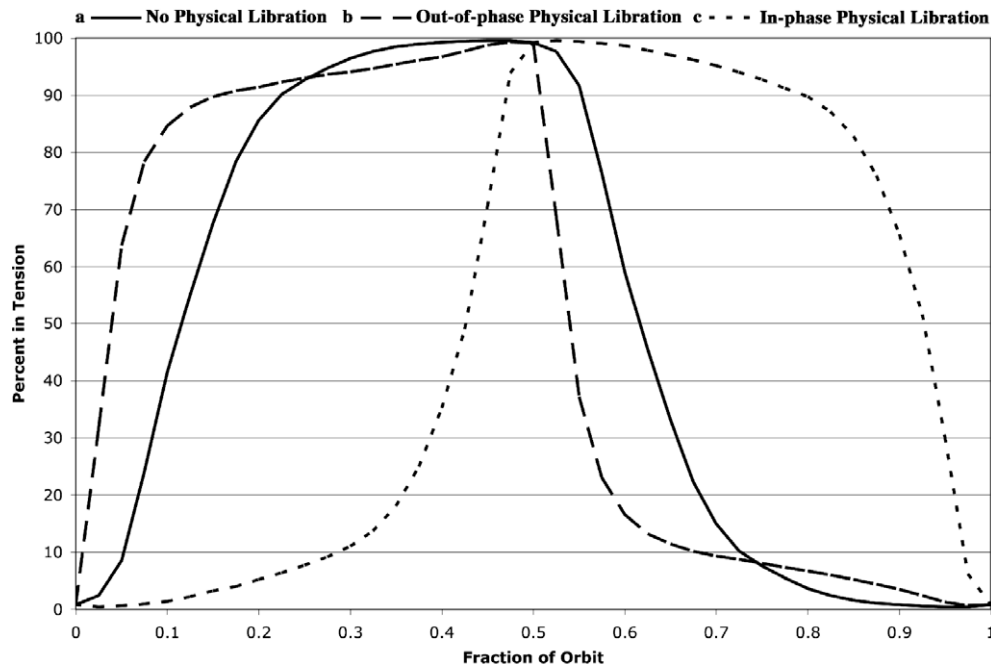


Fig. 5. The fraction of the tiger stripes in tension throughout the orbit for the cases in Fig. 1a–c. Eruption rates may be linked to the fraction of cracks in tension, creating variation in the plumes throughout the orbit. Different types of physical libration change the timing in when cracks experience tension and may also affect eruption rates throughout the orbit.

compression, which could affect the timing and location of eruptions. Fig. 4a shows the stresses on the tiger stripes during $\pi/4 < nt < \pi/2$ for the case with no physical libration (corresponding to Fig. 1a). During this period large portions of the tiger stripes are transitioning from compression to tension (shown by yellow in Fig. 4a). However, if Enceladus exhibits a physical libration, the timing of this transition changes. For example, in the case where the physical libration has an amplitude of $F = 1.5^\circ$ that is out of phase with the optical libration (Fig. 4b), during the same eighth of an orbit period most of the tiger stripes remain in tension, having transitioned from compression to tension during the period $0 < nt < \pi/4$. Finally, for the same physical libration amplitude, but in phase with the optical libration (Fig. 4c), the stresses on the tiger stripes during this part of the orbit are mostly compressive.

During each orbit, every portion of each tiger stripe rift spends roughly half the time in tension, which may expose volatiles and allow eruptions. Then, within a few hours, once again the stress becomes compressive, forcing cracks to close, ending any possibility of an eruption until the next cycle. Therefore, eruption rates may vary periodically, affecting the injection of material into Saturn's E ring.

In a simple model, eruption rates may be proportional to the total length of tiger stripe segments in tension at any moment. Fig. 5 shows the fraction of the tiger stripes in tension, our proxy for eruption rate, throughout the orbit for the three cases of Fig. 1. In the case of no libration, we would expect eruption rates to be high during the first half of the orbit and low during the second half. An out-of-phase physical libration could increase eruption activity even sooner in the orbit, since the tiger stripes open more quickly after pericenter passage. The opposite is seen for a physical libration that is in phase with the optical libration, leading to the possibility of more eruption activity during the second half of the orbit. Certain distributions of eruption activity, therefore, would be indicative of a physical libration of a given phase.

3.2. Tidal shear heating

While periodic stress across the tiger stripes may control eruption events, in a complementary process, periodic shear stress along the rifts may generate heat along their lengths (Nimmo and Gaidos, 2002; Prockter et al., 2005; Nimmo et al., 2007). The shear stress can drive strike–slip motion along the fault and in turn can dissipate energy through frictional heating. According to (Nimmo et al. (2007)), this additional source of heat may have the capacity to enhance eruptions, although that model depends on the assumed rate of strike–slip displacement.

In that model, heat generated by tidal shear stress along rifts in the south polar region of Enceladus have been compared with the locations of hotspots observed by Cassini's Composite Infrared Spectrometer (CIRS) (Spencer et al., 2006). There is a reasonable correlation between hotspot locations and predictions of tidal heat generation along the Damascus fault. However, on the Baghdad fault, CIRS detected the hottest region near the south pole, which does not fit the tidal shear heating model (Spencer et al., 2006; Nimmo et al., 2007).

The mismatch between the theory of tidal shear heating and the observations of heat on Enceladus may be due to over simplifications in the model of tidal shear heating by Nimmo et al. (2007). One possibility important effect that was neglected are physical librations which affect the diurnal tidal stress and therefore the amount of tidal shear heating along rifts.

Fig. 6 illustrates how a physical libration can affect tidal shearing along the tiger stripes. In Fig. 6a the amount of shear experienced along the tiger stripes is calculated in a similar method as was described by Nimmo et al. (2007), except we use a thin shell approximation for the diurnal tidal stress on Enceladus' surface. The results shown in Fig. 6a reproduce earlier results by Nimmo et al. (2007). However, when a physical libration is added the pattern of tidal shear changes, and hence the amount of heat generated and the locations of hot spots are also affected. In the case of the libration shown in Fig. 6b (physical

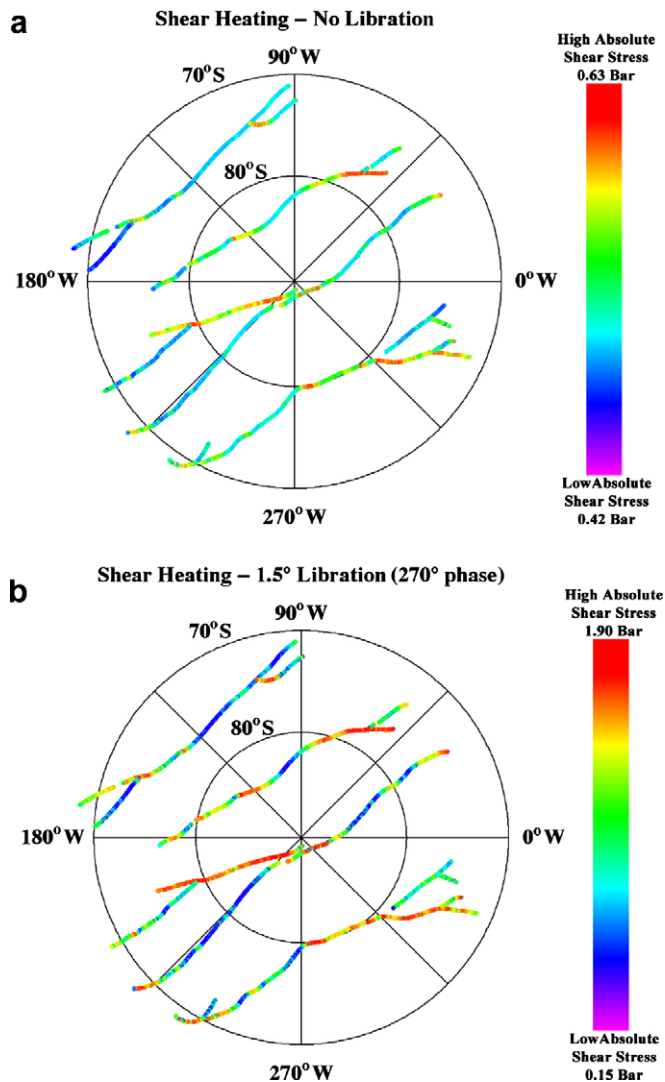


Fig. 6. Absolute tidal shear has been calculated along the tiger stripes in the south polar region for the case when Enceladus has (a) no physical libration and (b) a physical libration of amplitude 1.5° that has a phase of 270° . In the first case, our results match those of Nimmo et al. (2007). In the second case, areas of greater shearing shown in (a), and thus presumably the locations of hot spots, remain. However, more shearing is seen near the south pole along Baghdad, predicting more tidal shear heating in that region, which matches some aspects of CIRS observations better. Note: Each plot has a different dynamic range between hot and cold colors.

libration of 1.5° in amplitude with a phase of 270°), areas of high shearing seen in Fig. 6a are still present, but new areas of high shearing have emerged. While this particular libration amplitude and phase was chosen to illustrate the effect of a libration on tidal shear heating, our result with libration results in extra shear near the south pole, implying greater heating at that location, which would be a better match to the heat measured there by CIRS. This agreement provides indirect evidence (albeit model-dependent) that Enceladus may undergo physical libration. Various other combinations of libration amplitude and phase may also result in better matches to CIRS data and a systematic survey of the libration phase space could identify which librations best characterize the observations.

3.3. Strike-slip motion

In a method similar to that used to consider stress along cracks on Europa's surface, diurnal variation in the surface stress on a fault

can be calculated (Hoppa et al., 1999a). Tidal stress along a fault can produce strike-slip displacement by a process analogous to walking (Hoppa et al., 1999a). In tidal walking faults open and close out of phase with left- and right-lateral shear producing small, net, daily offsets along the faults. When the stress normal to a fault is tensile, the fault opens allowing shear stress to produce an offset. About half an orbit later, the stress normal to the fault changes from tension to compression, closing the fault. Once closed, friction along the fault limits the ability of shear stress to completely relieve the entire offset. After one cycle, the fault displays a small net sense of strike-slip displacement along its length. Over many successive cycles of opening and closing the small strike-slip offsets build, producing a greater amount of strike-slip displacement. Such displacements may ultimately be observed on Enceladus as well, with Cassini Imaging Science Subsystem (ISS) images.

The sense (left- or right-lateral) of strike-slip displacement along a fault depends predictably on the orientation and location of the fault, according to the tidal walking theory (Hoppa et al., 1999a). Without physical libration, strike-slip displacements poleward of 60°S should all be right-lateral in sense (Hoppa et al., 1999a) because stresses in this region rotate in a clockwise direction throughout Enceladus' orbit.

However, when we add the effect of physical libration, tidal walking can yield left-lateral strike-slip displacement in the south polar region (Fig. 7), if the amplitude of the physical libration is greater than the optical libration ($2e$ radians, i.e. $F > 0.54^\circ$) and the libration is relatively in phase. In such a case, the stress field throughout the orbit rotates in a counter-clockwise direction, allowing left-lateral strike-slip displacement.

A preliminary survey of strike-slip faults near Enceladus south pole has found tentative examples of both right- and left-lateral strike-slip displacements (Hurford et al., 2008). If we assume that the observed strike-slip offsets are caused by tidal stresses and have not been caused by regional tectonic stresses, this result indicates that the physical libration may have an amplitude at least as large as the amplitude of the optical libration (i.e. $F \geq 2e$ radians or 0.54°). If the relative phase between the physical and optical libration changes with time, right-lateral offsets would form along strike-slip faults when the two librations are relatively out of phase with each other, but left-lateral offsets would form when the two librations are in phase with each other (Fig. 7). If the amplitude of the physical libration were less than amplitude of the optical libration ($F < 2e$), only right lateral strike-slip offsets should be produced, regardless of the libration phase.

3.4. Initial formation of cracks

One prominent tiger stripe near Enceladus' south pole consists of arcuate segments, resembling the shape of cycloidal cracks on Europa (c.f. Hurford et al. (2007)). On Europa, these distinctive tectonic patterns were likely produced by periodic tidal stresses (Hoppa et al., 1999b). As the cracks form and propagate across the surface, their paths are altered as the stresses rotate in the region. The similarity between Enceladus' tiger stripes and Europa's cycloidal ridges is in shape only; they are quite distinct from one another morphologically. Nevertheless, the similar shape of the tiger stripe suggests that its formation may have been similarly controlled by diurnal tidal stresses (Hurford et al., 2006; Hurford et al., 2007; Nimmo et al., 2007). Subsequent modification of the surface along the tiger stripes on Enceladus likely differed from the ridge-forming processes on Europa.

On Enceladus, with just stress from the optical libration, the arcuate rift would not have formed at its current location (Hurford et al., 2006; Hurford et al., 2007). The variations in the stress field at this longitude cannot recreate the shape of the feature. As with Europa (Hoppa et al., 2001), the formation of the feature may pro-

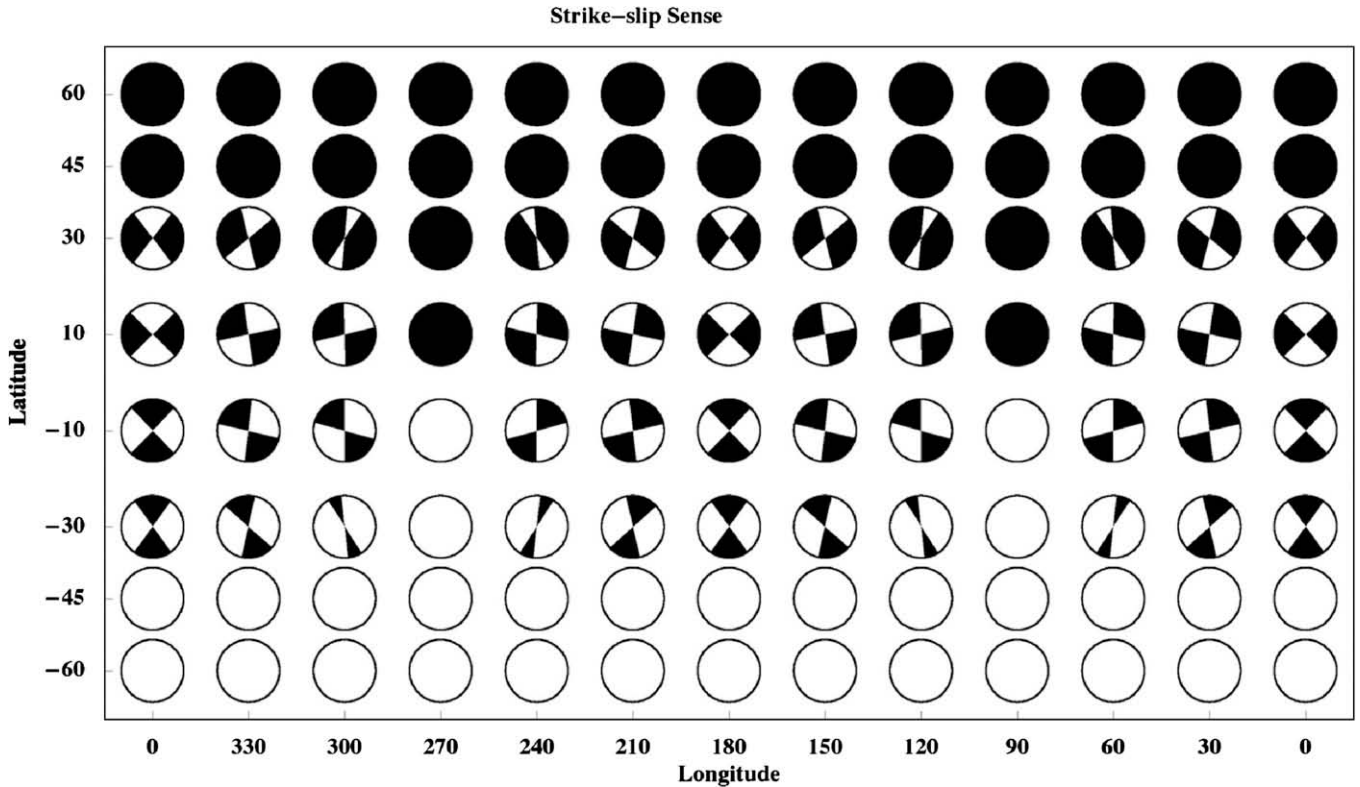


Fig. 7. This plot, used in conjunction with Fig. 3, shows the effect of libration on strike-slip displacement. Here right-lateral displacement is shown as white (left-lateral displacement as black) for values of the physical libration amplitude and phase that define the white region in Fig. 3. For parameters falling in the black region of Fig. 3, the meanings of white and black in this figure are reversed. Along the grey margin between white and black regions in Fig. 3 no strike-slip displacement occurs along any faults of any orientation.

vide evidence of where (relative to a Saturn centered reference frame) this feature might have formed, prior to subsequent rotation. However, This feature is one of the stratigraphically youngest (Helfenstein et al., 2009) active tiger stripes and it may have formed at its current location. Currently, models of crack formation have neglected the role of a physical libration in the calculation of tidal stress. Thus, if this tiger stripe did form at its current location, the modeling of its formation, assuming a physical libration, may provide further evidence for Enceladus' libration state.

4. Global tidal dissipation

A physical libration was first invoked in order to provide greater amounts of heat to the system by allowing Enceladus to tidally dissipate more energy (Wisdom, 2004). The tidal heating is given by

$$\frac{dE}{dt} = \left[\frac{9}{2}e^2 + \frac{3}{2}(2e + F)^2 + \frac{3}{8}S^2 + \frac{3}{2}(\sin \varepsilon)^2 \right] \frac{k_2}{Q} \frac{GM^2 n R^5}{a^6} \quad (4)$$

where S is the amplitude of the secondary forced libration, assuming that Enceladus is near the 4:1 secondary spin-orbit resonance (Peale and Cassen, 1978, 2004). Wisdom (2004) assumed that the physical libration, F , is out of phase with the optical libration. Thus a more general expression of tidal heating (sans our assumptions) would be

$$\frac{dE}{dt} = \left[\frac{9}{2}e^2 + \frac{3}{2}L^2 + \frac{3}{8}S^2 + \frac{3}{2}(\sin \varepsilon)^2 \right] \frac{k_2}{Q} \frac{GM^2 n R^5}{a^6} \quad (5)$$

where $L = \sqrt{4e^2 + F^2 - 4eF \cos(\psi)}$, which is the amplitude of the oscillation in the longitude of the tidal bulge described by $-2e \sin(nt) + F \sin(nt + \psi)$. When $\psi = \pi$, $L = 2e + F$ which is the value assumed by Wisdom (2004). If we neglect possible secondary

librations ($S = 0$) and assume zero obliquity ($\varepsilon = 0$), then the factor by which tidal dissipation is modified can be expressed as

$$f_H = \frac{3e^2 + L^2}{7e^2}. \quad (6)$$

The physical libration can enhance or retard tidal dissipation, depending on the value of L (Fig. 8). For cases when $L < 2e$ tidal dissipation is retarded. In fact f_H has a minimum value of 0.43 when $L = 0$. Enhancement of tidal dissipation occurs when $L > 2e$. If Enceladus' physical libration remains constant in amplitude but slowly migrates in phase over time (a condition that can happen if the libration period is slightly off the orbital period), Enceladus can experience periodic episodes of heating and cooling.

The most enhancement of tidal heating occurs for the case of a physical libration at the Cassini's limit of $L = 1.5^\circ$. In this case the tidal heating is enhanced by ~ 4.9 times. Given recent work by Hurford et al. (2007) and Nimmo et al. (2007), which imply at least 8 GW of tidal heating, Enceladus could be dissipating ~ 40 GW, making the ~ 6 GW seen in the south polar region only a small fraction of the total heat supplied to the system.

5. Discussion

We have shown that a physical libration may have profound effects on geological processes in which tidal stress plays a dominant role. Observations of eruption activity, heat distributions, tectonic displacement and crack shapes (Sections 3.1–3.4, respectively) may provide indirect evidence of Enceladus' physical libration. In addition, the Cassini spacecraft provides a platform with several different instruments, especially ISS, that may be able to detect any physical libration.

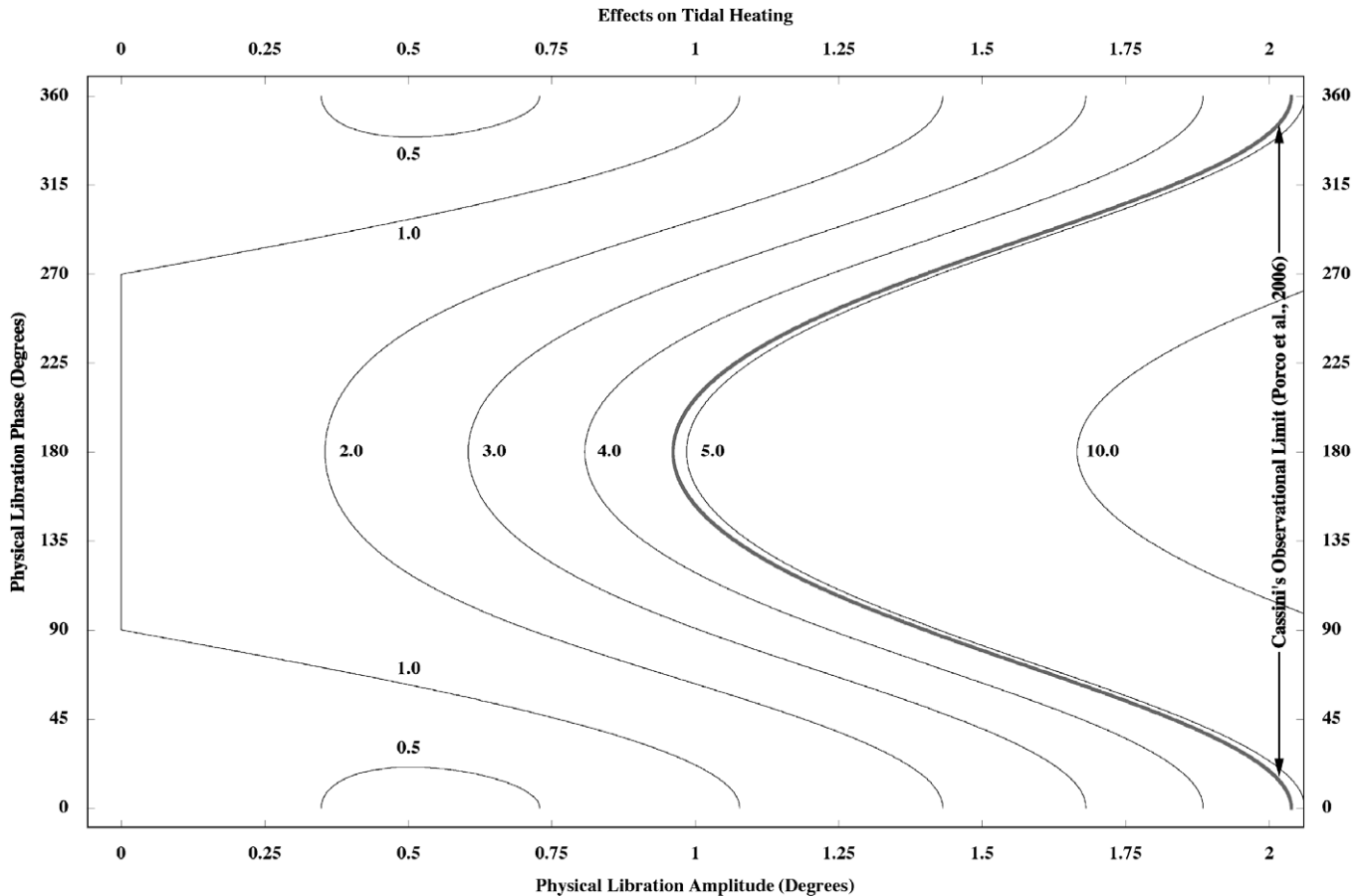


Fig. 8. The factor f_H (Eq. (6)) by which heating is affected is calculated for different values of the physical libration amplitude and its phase relative to the optical libration. In most cases tidal heating is enhanced ($f_H > 1$) by the presence of a physical libration; the heating is minimum $f_H = 0.43$ for an in-phase physical libration ($\psi = 0^\circ$) with amplitude $F = 2e = 0.54^\circ$.

Observations of the eruption activity on Enceladus provide the best way to detect Enceladus' current libration state (Section 3.1). Cassini ISS can directly detect the plumes during high phase imaging. Multiple images, with Enceladus at different points in its orbit, may provide evidence that the eruption rates from Enceladus' south pole vary with orbital position. Cassini UVIS, INMS and MAG observations can also provide constraints on the eruption rates and their variability (Hansen et al., 2008; Saur et al., 2008). As those data become available we can expand on the results of Section 3.1. The changing eruption rates and distribution can be compared to models of how tidal stresses facilitate eruptions, providing more information about the physical libration.

Observations of heat distributions on Enceladus' south polar region can also be used to detect Enceladus' current libration state (Section 3.2). Cassini CIRS detects the surface temperatures on Enceladus. Tidal shear heating depends on the diurnal stress field, which is affected by a physical libration. Models of tidal shear heating may be able to match the locations of high temperatures observed by CIRS. Current models cannot produce enough heat on Baghdad but future models, which incorporate a physical libration may better match the CIRS data.

Finally, observations of the geology of the south polar region can provide evidence of Enceladus' physical libration (Sections 3.3 and 3.4). Cassini ISS has provided detailed images of the south polar terrain. Modeling the formation of cracks, such as the cycloidal tiger stripe, and strike-slip displacements may provide evidence that a physical libration is needed to best reproduce these features. However, the additional stress from a physical libration affected these features at the time of their formation, and if the

libration state changes with time, it may not be the same for each observation or for that matter may not be the same as the current libration state.

All these observational techniques together provide independent methods of characterizing Enceladus' physical libration state. Fig. 9 shows a sketch of these processes and the intersection of their results. Physical libration states that can explain the most observations are more likely to exist. Only by systematically studying each process on its own, can a comprehensive understanding of Enceladus' rotation state can be made.

Although we have focused on Enceladus, physical librations of satellites may be common in the solar system. Recently, work has suggested that winds on Titan may be able to drive a forced libration of Titan's surface (Tokano and Neubauer, 2005), if Titan has a liquid ocean that can decouple its surface from the interior. Moreover, possible interpretations of Cassini RADAR observations hint that this type of forced libration may exist on Titan (Lorenz et al., 2008). On Europa, the icy crust is almost certainly decoupled from the deeper interior. Recent studies have speculated about the possibility that it also exhibits a spin-orbit libration as tidal torques from Jupiter may be able to force this ice shell to librate (van Hoolst et al., 2008). Such physical librations on Titan and on Europa, as with Enceladus, could alter tidal stress fields, which would influence geological processes on their surfaces.

6. Conclusions

Current efforts to directly detect Enceladus' physical libration limits its amplitude to $\leq 1.5^\circ$. However, future observations by Cas-

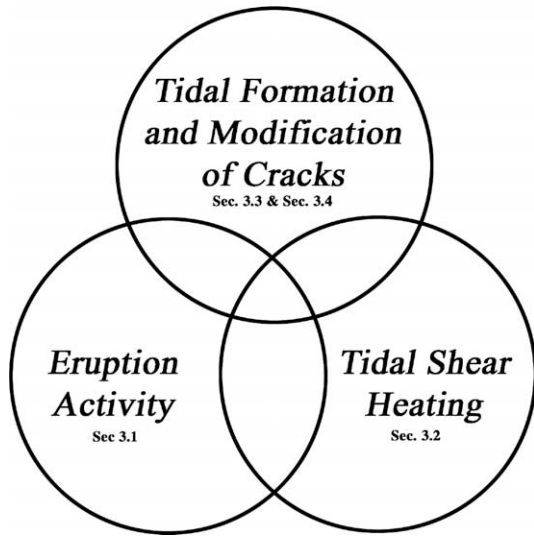


Fig. 9. Possible consequences of the libration of Enceladus. If some or all of these processes are controlled by libration, they could provide powerful constraints on the amplitude and phase of this motion.

sini may place more stringent limits on its amplitude and perhaps may even detect the libration. Libration can be directly detected by observing slight changes in the location of surface features with respect to (a) the terminator, (b) the limb or (c) the spin pole. Detections with respect to the terminator are difficult because topography can obscure the true location of a feature and limb observations suffer from foreshortening. Thus observations of change with respect to the spin pole provide the best chance of observing Enceladus' libration. In order to see the effect of Enceladus' libration a higher resolution control grid, able to detect changes to less than 1° , will be needed.

The effect of a libration, if it exists, may be profound on diurnal tidal stress. A change in the diurnal stress will in turn affect geological processes controlled by these stresses. The location and timing of eruptions will be affected as will the heat generated by tidal shear heating. The formation and modification of cracks on the surface will also be influenced by the stress produced by a physical libration. The ramifications of the diurnal stress on geological processes are more easily observable and may provide the best and only way to indirectly detect Enceladus' librational state. Observations of each process can provide its own unique constraint on the libration amplitude and phase. A robust case for physical libration would result if a single model could be constructed to simultaneously account for several geological processes.

Acknowledgments

This work was supported by NASA Grants issued to T.H. and P.H. through the Cassini Data Analysis Program.

Appendix A. Diurnal tidal stress on a librating body

Variation in the tidal figure of a moon as it orbits its primary produces stress on its surface on a diurnal timescale. The diurnal tidal stress, σ^D , driven by optical libration (the effects of orbital eccentricity and obliquity) and physical libration, is the difference between the instantaneous tidal stress, $\sigma(t)$, produced by Europa's tidal figure caused by eccentricity and obliquity at any point in its orbit and the time invariant tidal stress, σ , represented by its average tidal deformation. The diurnal tidal stress is

$$\sigma^D = \sigma(t) - \sigma = \begin{bmatrix} \sigma(t)_{xx} - \sigma_{xx} & \sigma(t)_{xy} - \sigma_{xy} \\ \sigma(t)_{yx} - \sigma_{yx} & \sigma(t)_{yy} - \sigma_{yy} \end{bmatrix}. \quad (7)$$

The stress tensors $\sigma(t)$ and σ , written in terms of principal stresses, have different orientations and must be transposed such that their components describe the tidal stress in a common reference frame. Stress in the xx direction is aligned east-west while in the yy direction it is north-south.

The principal components of the time invariant tidal stresses at any latitude δ and longitude λ , produced by the thin shell approximation of stress σ , are given by Eqs. (1) and (2) with $\theta = \cos^{-1}[\cos \delta \cos \lambda]$ (longitude is defined as positive to the west). The components of the stress tensor σ are

$$\sigma_{xx} = \frac{1}{2}(\sigma_{\phi\phi} + \sigma_{\theta\theta}) - \frac{1}{2}(\sigma_{\phi\phi} - \sigma_{\theta\theta}) \cos 2\beta, \quad (8)$$

$$\sigma_{yy} = \frac{1}{2}(\sigma_{\phi\phi} + \sigma_{\theta\theta}) + \frac{1}{2}(\sigma_{\phi\phi} - \sigma_{\theta\theta}) \cos 2\beta, \quad \text{and} \quad (9)$$

$$\sigma_{xy} = \sigma_{yx} = -\frac{1}{2}(\sigma_{\phi\phi} - \sigma_{\theta\theta}) \sin 2\beta \quad (10)$$

where the angle β describes the tilt of the principal stress axis with respect to the common reference frame and has the value

$$\beta = \cos^{-1} \left[-\frac{\sin \delta \cos \theta}{\cos \delta \sin \theta} \right]. \quad (11)$$

The angle β is the angle subtended by the north pole of the body, the location at which the stress is being evaluated (δ, λ) and the location of the average sub-planet point on the surface (0,0).

The principal components of the instantaneous tidal stresses, $\sigma(t)$, caused by the change in tidal figure due to optical and physical librations at any point in the orbit, are given by modified forms of Eqs. (1) and (2), which are valid when e is small (i.e. the tidal magnitude changes by $(1 - e \cos nt)^{-3} \approx (1 + 3e \cos nt)$,

$$\sigma(t)_{\theta\theta} = \frac{3M\mu h_2}{8\pi\rho_{av}a^3} \left(\frac{1+\nu}{5+\nu} \right) (5 + 3 \cos 2\theta(t))(1 + 3e \cos nt) \quad (12)$$

and

$$\sigma(t)_{\phi\phi} = -\frac{3M\mu h_2}{8\pi\rho_{av}a^3} \left(\frac{1+\nu}{5+\nu} \right) (1 - 9 \cos 2\theta(t))(1 + 3e \cos nt), \quad (13)$$

where the tidal height and bulge location vary because of the orbital eccentricity e based on the angular position in the orbit defined by nt , such that n is the mean motion and t time in seconds after pericenter passage. Moreover, the instantaneous angular distance, $\theta(t)$, between any point on the surface (δ, λ) and the instantaneous location of the tidal bulge is time dependent and described by

$$\theta(t) = \cos^{-1}[\sin \delta \sin(\varepsilon \sin(nt - \omega)) + \cos \delta \cos(\varepsilon \sin(nt - \omega)) \cos(\lambda + 2e \sin(nt) - F \sin(nt + \psi))] \quad (14)$$

where ε is the obliquity, ω is the angle between the direction of the ascending node and the direction of pericenter and F is the amplitude of the physical libration with phase ψ . Here we focus on the physical libration that is driven at the orbital frequency, free librations may occur at frequencies other than the orbital frequency and those librations can be added to $\theta(t)$ by adding terms similar to $-F \sin(nt + \psi)$ which describe the free librations.

The components of the stress tensor $\sigma(t)$ are

$$\sigma_{xx}(t) = \frac{1}{2}(\sigma_{\phi\phi}(t) + \sigma_{\theta\theta}(t)) - \frac{1}{2}(\sigma_{\phi\phi}(t) - \sigma_{\theta\theta}(t)) \cos 2\beta(t), \quad (15)$$

$$\sigma_{yy}(t) = \frac{1}{2}(\sigma_{\phi\phi}(t) + \sigma_{\theta\theta}(t)) + \frac{1}{2}(\sigma_{\phi\phi}(t) - \sigma_{\theta\theta}(t)) \cos 2\beta(t), \quad \text{and} \quad (16)$$

$$\sigma_{xy}(t) = \sigma_{yx}(t) = -\frac{1}{2}(\sigma_{\phi\phi}(t) - \sigma_{\theta\theta}(t)) \sin 2\beta(t) \quad (17)$$

where the angle $\beta(t)$ describes the tilt of the instantaneous principal stress axis with respect to the common reference frame and is defined as

$$\beta(t) = \cos^{-1} \left[\frac{\sin(\varepsilon \sin(nt - \omega)) - \sin \delta \cos \theta(t)}{\cos \delta \sin \theta(t)} \right]. \quad (18)$$

The angle $\beta(t)$ is the angle subtended by the north pole of the body, the location at which the stress is being evaluated (δ, λ) and the instantaneous location of the sub-planet point on the surface.

With the formulation of σ and $\sigma(t)$ in similar reference frames, the diurnal stress, σ^D , can now be evaluated. It is often convenient to express the diurnal stress tensor in terms of the principal stresses, such that shear stresses are zero,

$$\sigma^D = \begin{vmatrix} \sigma_1^D & 0 \\ 0 & \sigma_2^D \end{vmatrix}. \quad (19)$$

The principal stresses are

$$\sigma_1^D = \sigma_{xx}^D \cos^2 \gamma_D + \sigma_{yy}^D \sin^2 \gamma_D + \sigma_{xy}^D \sin 2\gamma_D \quad (20)$$

and

$$\sigma_2^D = \sigma_{xx}^D \sin^2 \gamma_D + \sigma_{yy}^D \cos^2 \gamma_D - \sigma_{xy}^D \sin 2\gamma_D \quad (21)$$

where γ describes the orientation of the principal stress axis and is given by

$$\gamma_D = \frac{1}{2} \tan^{-1} \left[\frac{2\sigma_{xy}^D}{\sigma_{xx}^D - \sigma_{yy}^D} \right]. \quad (22)$$

The angle, γ_D is measured from the σ_{xx}^D direction to the σ_1^D direction.

References

Greenberg, R., 2005. Europa—The Ocean Moon: Search for an Alien Biosphere. Springer-Verlag (Springer-Praxis Books in Geophysical Sciences Series), Berlin.

Greenberg, R., Geissler, P., Hoppa, G., Tufts, B.R., Durda, D.D., Pappalardo, R., Head, J.W., Greeley, R., Sullivan, R., Carr, M.H., 1998. Tectonic processes on Europa: Tidal stresses, mechanical response, and visible features. *Icarus* 135, 64–78.

Hansen, C.J., Esposito, L., Colwell, J., Hendrix, A., Meinke, B., Stewart, I., 2008. New occultation observation of Enceladus' plume. In: Lunar and Planetary Institute Conference Abstracts, Vol. 39 of Lunar and Planetary Inst. Technical Report. 2014pp.

Helfenstein, P., and 13 colleagues. 2009. Tectonism and terrain evolution on enceladus. *Icarus*.

Hoppa, G., Tufts, B.R., Greenberg, R., Geissler, P., 1999a. Strike-slip faults on Europa: Global shear patterns driven by tidal stress. *Icarus* 141, 287–298.

Hoppa, G.V., Randall Tufts, B., Greenberg, R., Hurford, T.A., O'Brien, D.P., Geissler, P.E., 2001. Europa's rate of rotation derived from the tectonic sequence in the Astypalaea region. *Icarus* 153, 208–213.

Hoppa, G.V., Tufts, B.R., Greenberg, R., Geissler, P.E., 1999b. Formation of cycloidal features on Europa. *Science* 285, 1899–1902.

Hurford, T.A., Bills, B.G., Greenberg, R., Hoppa, G.V., Helfenstein, P., 2008. How libration affects strike-slip displacement on Enceladus. In: Lunar and Planetary Institute Conference Abstracts, Volume 39 of Lunar and Planetary Institute Conference Abstracts, 1826pp.

Hurford, T.A., Greenberg, R., Hoppa, G.V., 2006. South Polar Cycloidal Rift on Enceladus. In: AAS/Division for Planetary Sciences Meeting Abstracts. 18.04pp.

Hurford, T.A., Helfenstein, P., Greenberg, R., Hoppa, G.V., 2007. A Cycloid-like Rift Near Enceladus' South Pole: Europa-style Production by Tidal Stress. In: Lunar and Planetary Institute Conference Abstracts, Volume 38 of Lunar and Planetary Institute Conference Abstracts. 1844pp.

Hurford, T.A., Helfenstein, P., Hoppa, G.V., Greenberg, R., Bills, B., 2007. Eruptions arising from tidally controlled periodic openings of rifts on Enceladus. *Nature* 447, 292–294.

Hurford, T.A., Sarid, A.R., Greenberg, R., 2007. Cycloidal cracks on Europa: Improved modeling and non-synchronous rotation implications. *Icarus* 186, 218–233.

Leith, A.C., McKinnon, W.B., 1996. Is there evidence for Polar Wander on Europa? *Icarus* 120, 387–398.

Lorenz, R.D., Stiles, B.W., Kirk, R.L., Allison, M.D., Persi del Marmo, P., Iess, L., Lunine, J.I., Ostro, S.J., Hensley, S., 2008. Titan's rotation reveals an Internal Ocean and Changing Zonal Winds. *Science* 319, 1649.

Melosh, H.J., 1977. Global tectonics of a despun planet. *Icarus* 31, 221–243.

Newton, I., 1686. *Philosophiae naturalis principia mathematica*. Lib. III, Prop. 17 and 38. London.

Nimmo, F., Gaidos, E., 2002. Strike-slip motion and double ridge formation on Europa. *J. Geophys. Res. (Planets)* 107, 5.

Nimmo, F., Spencer, J.R., Pappalardo, R.T., Mullen, M.E., 2007. Shear heating as the origin of the plumes and heat flux on Enceladus. *Nature* 447, 289–291.

Peale, S.J., Cassen, P., 1978. Contribution of tidal dissipation to lunar thermal history. *Icarus* 36, 245–269.

Porco, C.C., Helfenstein, P., Thomas, P.C., Ingersoll, A.P., Wisdom, J., West, R., Neukum, G., Denk, T., Wagner, R., Roatsch, T., Kieffer, S., Turtle, E., McEwen, A., Johnson, T.V., Rathbun, J., Veverka, J., Wilson, D., Perry, J., Spitale, J., Brahic, A., Burns, J.A., DelGenio, A.D., Dones, L., Murray, C.D., Squyres, S., 2006. Cassini observes the active South Pole of Enceladus. *Science* 311, 1393–1401.

Prockter, L.M., Nimmo, F., Pappalardo, R.T., 2005. A shear heating origin for ridges on Triton. *Geophys. Res. Lett.* 32, L14202.

Saur, J., Schilling, N., Fritz, N., Darrell, F., Simon, S., Dougherty, M., Russell, C., 2008. Evidence for temporal variability of Enceladus' gas jets: Modeling of Cassini observations. *GRL* in review 000, 000.

Schubert, G., Spohn, T., Reynolds, R.T. 1986. Thermal histories, compositions and internal structures of the Moons of the Solar system, pp. 224–292. *IAU Colloq. 77: Some Background about Satellites*.

Sohl, F., Hussmann, H., Ziethe, R., 2006. Interior Structures of Enceladus and Mimas: Implications from their densities and equilibrium shapes. *Bull. Am. Astron. Soc.* 38, 521.

Spencer, J.R., Pearl, J.C., Segura, M., Flasar, F.M., Mamoutkine, A., Romani, P., Buratti, B.J., Hendrix, A.R., Spilker, L.J., Lopes, R.M.C., 2006. Cassini encounters Enceladus: Background and the discovery of a south polar hot spot. *Science* 311, 1401–1405.

Spitale, J.N., Porco, C.C., 2007. Association of the jets of Enceladus with the warmest regions on its south-polar fractures. *Nature* 449, 695–697.

Thomas, P.C., Burns, J.A., Helfenstein, P., Squyres, S., Veverka, J., Porco, C., Turtle, E.P., McEwen, A., Denk, T., Giese, B., Roatsch, T., Johnson, T.V., Jacobson, R.A., 2007. Shapes of the saturnian icy satellites and their significance. *Icarus* 190, 573–584.

Tokano, T., Neubauer, F.M., 2005. Wind-induced seasonal angular momentum exchange at Titan's surface and its influence on Titan's length-of-day. *GRL* 32, 24203.

van Hoolst, T., Rambaux, N., Karatekin, Ö., Dehant, V., Rivoldini, A., 2008. The librations, shape, and icy shell of Europa. *Icarus* 195, 386–399.

Wisdom, J., 2004. Spin-orbit secondary resonance dynamics of Enceladus. *Astron. J.* 128, 484–491.

Yoder, C.F., 1979. How tidal heating in Io drives the Galilean orbital resonance locks. *Nature* 279, 767–770.

Zhang, K., Nimmo, F., 2009. Internal structure of Enceladus and Dione from Orbital constraints. In: Lunar and Planetary Institute Science Conference Abstracts, Volume 40 of Lunar and Planetary Institute Science Conference Abstracts. 2199pp.